Journal of Computational Physics **175,** 225–248 (2002)
doi:10.1006/jcph.2001.6940, available online at http://www.idealibrary.com on IDEAL®

Tests of a Simulation Method for Boltzmann-like Models with Chemical Reactions

Dorin Marinescu,* Aude Espesset,† and Cecil P. Grünfeld‡

*Institute of Applied Mathematics, Romanian Academy, Calea 13 Septembrie, No. 13, Sector 5, P.O. Box 1-24, 70700, Bucharest, Romania; †National Institute of Applied Sciences of Toulouse, Scientific Complex of Rangueil, 31077 Toulouse Cedex 4, France; and ‡Institute of Space Sciences, INFLPR, P.O. Box MG-23, Bucharest-Măgurele, Romania

E-mail: *dorinm@iacob.ima.ro, †espesset@gmm.insa-tlse.fr, and ‡grunfeld@ifin.nipne.ro

Received November 29, 2000; revised July 2, 2001

This paper reports on the numerical implementation of a convergent scheme solving a general class of nonlinear Boltzmann-like equations for reacting fluids. The scheme is tested on a model of space-homogeneous multicomponent gas with binary chemical reactions. Although the model cannot be solved exactly, it provides analytical expressions for certain low-order moments of the one-particle distribution functions. Computing these moments by applying the numerical scheme, one obtains a good agreement with the values obtained analytically. An error analysis is performed and error control considerations complete the theoretical support of the scheme developed in previous works. © 2002 Elsevier Science

Key Words: numerical simulation; gas mixtures; chemical reactions; Boltzmann equation; Monte-Carlo methods.

1. INTRODUCTION

Accurate numerical modeling of nonlinear processes in dilute, reacting flows is critical for solving transport problems both in fundamental and applied science, e.g., in astrophysics, physics and chemistry of planetary atmospheres, technology of space vehicles, combustion, chemical reactors, etc. In this respect, the past few years have been marked by considerable progress in the development of algorithms for Boltzmann models. Since there are many excellent textbooks and well-documented papers, a review on this topic is beyond the scope of our work. From the multitude of papers, here we only mention a few successful recent approaches to describing various reacting gas regimes: iterative linear Boltzmann transport schemes [3], splitting algorithm for the BGK model with chemical reactions [11], lattice BGK schemes for reacting fluids [16], and lattice gas automata methods [2]. A summary of the literatures shows that the competitiveness of various methods is open and opinions are still divided.

0021-9991/02 $35.00
© 2002 Elsevier Science
All rights reserved.

To avoid mathematical difficulties, in many situations where dilute reacting fluids are (considered as) properly described by nonlinear Boltzmann models, the numerical schemes are actually applied to simplified reformulations of the models, e.g., obtained by linearization of the collision operators. Nevertheless, there are physical processes, such as far-from-equilibrium kinetic stages, where a more realistic description has to take into account the effects of the nonlinearities of the Boltzmann collision operators.

As a result, there is increased interest [17] in precise numerical methods for nonlinear Boltzmann models (with unaltered collision operators) able to describe the complexity of phenomena specific to these type of equations.

In this respect, a rigorous numerical scheme has been recently introduced [7] to solve a general class of nonlinear Boltzmann-like equations [5, 6] for dilute chemically reacting fluids. This scheme extends an efficient, so-called particle method, developed by Nambu [14] and Babovsky and Illner [1] (NBI), which combines analytical and stochastic techniques into a convergent algorithm for the classical Boltzmann equation (for the simple gas).

To extend the NBI method by including chemical reactions, one has to face new mathematical difficulties, because of the presence of several species and threshold conditions in the energetic balance, which imply more complications in the structure of the collision operators, than for the simple gas. Since the collision operators are acting only on the velocity-dependent part of the one-particle distribution functions, these difficulties are already encountered in the treatment of the simpler, space-homogeneous reacting fluids. For such fluids, the method considers a time-discretized version of the Boltzmann model (keeping the collision operators in their original forms) and introduces an iteration scheme that converges, in some sense, to the solution of the Boltzmann equation, when the discretization time step decreases to zero. The main benefit is that, using the properties of the collision operators, the method provides a weak form of the iteration, which can be solved exactly in the positive cone of discrete measures (defined on the velocity space, in our case). Applying low-discrepancy techniques [9] to approximate (with arbitrary accuracy) the general initial data by means of discrete measures, the above analytic procedure results in a convergent scheme for the general solutions of the nonlinear Boltzmann equation. However, the nonlinearities imply a power-like increasing computational effort at each iteration step. This is the stage when the stochastic element is invoked, its role being only to keep the numerical effort unchanged. Specifically, at each iteration step, one uses random selection to diminish the number of points supporting the input discrete measure. The final algorithm is shown to converge almost everywhere to the true solution of the Boltzmann equation, in general, with a numerical effort of order $O(n \log n)$, as a consequence of the law of large numbers for arrays of random variables.

The generalization of this scheme to modeling space-dependent fluids seems rather a technical problem [7] and should follow essentially the same procedure as in [1], alternating convection steps with collision steps, in disjoint locally homogeneous space cells.

The potential advantage of the method is a more accurate calculation of the distribution functions and implicitly of the macroscopic properties, evaluated by integrals (averages) of various physical quantities with respect to the measures defined by the distribution functions.

Since most applications concern phenomena in nonhomogeneous fluids, the applicability of the method should be ultimately tested on those situations. However, this seems rather a difficult task since, in those cases, neither sufficient experimental data nor analytical solutions are available for confrontation with numerical results.

On the other hand, by virtue of the above considerations, numerical experiments on space-independent models with exact solutions can provide useful illustrations of the convergence of the method, error behavior, and robustness (having in mind the effects due to the presence of reactive collision terms). Moreover, unlike the situation of a simple gas, the study of a space-homogeneous reacting fluid could present intrinsic interest in certain cases, where one is led to dynamical systems with nontrivial behavior [12].

The scheme of [7] was tested in [13] on the exact Krook–Wu solutions [8] of the multicomponent Boltzmann equation. Since the Krook–Wu equations refer only to nonreactive gases, the results have not clarified the applicability of the method to models with chemical reactions. Unfortunately, even in the space-independent case, the known exact solutions of nonlinear Boltzmann models with chemical reactions are too simple to be of interest in testing the above scheme. However, indirect tests can be performed on certain models for space-homogeneous reacting fluids, which cannot be solved analytically, but provide exactly solvable equations for the time evolution of certain macroscopic variables (e.g., concentration, energy). In this case, the macroscopic quantities calculated by means of the numerical one-particle distribution functions (supplied by the scheme of [7]) can be compared with those obtained analytically.

The aim of this paper is to present the results of such an indirect test, which, although applied to a particular model, reveals the main features of the method. A detailed error analysis is included and general error estimations are obtained completing the theoretical developments of [7].

The implementation of the numerical method on the chosen model is performed in a more efficient way than in [13] owing to a slightly improved procedure. Roughly speaking, for each species, the number of concentration points of each discrete measure approximating the one-particle distribution function is kept proportional to the concentration.

The paper is organized as follows. Section 2 introduces the specific kinetic equations for analysis. The equations describe a gaseous mixture of (at most) four species of particles, with one-state internal energy and binary nonreactive or/and reactive collisions. Section 3 details theoretical considerations concerning the application of the numerical scheme to the equations introduced in Section 2. The numerical results of the tests and the error analysis are presented in Section 4. The last section is devoted to conclusions.

2. GAS MODEL WITH TWO KINDS OF CHEMICAL REACTIONS

In this paper we refer to a particular form of the model presented in [5, 6]. In detail, we consider a space-homogeneous gas mixture, composed of N species $X_1, \ldots, X_N$ of point particles with mass m_i, having one internal state characterized by a defined value of the internal energy E_i, $1 \le i \le N$. The gas particles undergo binary nonreactive collisions as well as reactions induced by binary collisions

$$X_i + X_j \to X_k + X_l, \quad 1 \le i, j, k, l \le N. \tag{1}$$

According to the model, reactions of the form (1) can occur only if the microscopic conservation of mass, momentum, and energy is fulfilled; i.e.,

$$m_i + m_j = m_k + m_l, \tag{2}$$

$$m_i \mathbf{v} + m_j \mathbf{w} = m_k \mathbf{v}' + m_l \mathbf{w}', \tag{3}$$

$$\frac{m_i|\mathbf{v}|^2}{2} + E_i + \frac{m_j|\mathbf{w}|^2}{2} + E_j = \frac{m_k|\mathbf{v}'|^2}{2} + E_k + \frac{m_l|\mathbf{w}'|^2}{2} + E_l, \tag{4}$$

where $\mathbf{v}$ and $\mathbf{w}$ are the precollision velocities of the particles i and j, and $\mathbf{v}'$ and $\mathbf{w}'$ are the postcollision velocities of the particles k and l, respectively.

Following, e.g., [5], it can be easily seen that, in the spatially homogeneous case, the one-particle distribution functions $f_i = f_i(t, \mathbf{v})$ describing the species $1 \le i \le N$, at moment $t \ge 0$, are solutions of the system of equations

$$\frac{\partial}{\partial t} f_i = P_i(\mathbf{f}) - S_i(\mathbf{f}), \quad 1 \le i \le N, \tag{5}$$

with the gain and loss terms P_i and S_i given by

$$P_i(\mathbf{f})(t, \mathbf{v}) := \sum_{j,k,l=1}^{N} \int_{\mathcal{D}_{ij;kl}(\mathbf{v})\times\mathbb{S}} p_{kl;ij}(\mathbf{v}, \mathbf{w}, \mathbf{n})\, f_k(t, \mathbf{v}_{ij;kl})\, f_l(t, \mathbf{w}_{ij,kl})\, d\mathbf{w}\, d\mathbf{n} \tag{6}$$

$$S_i(\mathbf{f})(t, \mathbf{v}) := f_i(t, \mathbf{v}) \sum_{j,k,l=1}^{N} \int_{\mathcal{D}_{ij;kl}(\mathbf{v})\times\mathbb{S}} r_{kl;ij}(\mathbf{v}, \mathbf{w}, \mathbf{n})\, f_j(t, \mathbf{w})\, d\mathbf{w}\, d\mathbf{n}. \tag{7}$$

In (5), (6), and (7), $\mathbf{f} := (f_1, \dots, f_N)$, $\mathbb{S} := \{\mathbf{n} \in \mathbb{R}^3 \mid |\mathbf{n}| = 1\}$, and $\mathcal{D}_{ij;kl}(\mathbf{v}) = \{\mathbf{w} \in \mathbb{R}^3 \mid (\mathbf{v}, \mathbf{w}) \in \mathcal{D}_{ij;kl}\}$, where

$$\mathcal{D}_{ij;kl} := \{(\mathbf{v}, \mathbf{w}) \in \mathbb{R}^3 \times \mathbb{R}^3 \mid \bar{W}_{ij;kl}(\mathbf{v}, \mathbf{w}) \ge 0\}, \tag{8}$$

with

$$\bar{W}_{ij;kl}(\mathbf{v}, \mathbf{w}) := \frac{m_i m_j}{2(m_i + m_j)}|\mathbf{v} - \mathbf{w}|^2 + E_i + E_j - E_k - E_l \tag{9}$$

and

$$\mathbf{v}_{ij;kl} = \mathbf{v}_{ij;kl}(\mathbf{v}, \mathbf{w}, \mathbf{n}) := \frac{m_i\mathbf{v} + m_j\mathbf{w}}{m_i + m_j} + \left[\frac{2 \cdot m_l}{m_k(m_i + m_j)}\bar{W}_{ij;kl}(\mathbf{v}, \mathbf{w})\right]^{1/2} \cdot \mathbf{n}, \tag{10}$$

$$\mathbf{w}_{ij;kl} = \mathbf{w}_{ij;kl}(\mathbf{v}, \mathbf{w}, \mathbf{n}) := \frac{m_i\mathbf{v} + m_j\mathbf{w}}{m_i + m_j} - \left[\frac{2 \cdot m_k}{m_l(m_i + m_j)}\bar{W}_{ij;kl}(\mathbf{v}, \mathbf{w})\right]^{1/2} \cdot \mathbf{n}, \tag{11}$$

for all $(\mathbf{v}, \mathbf{w}, \mathbf{n}) \in \mathcal{D}_{ij;kl} \times \mathbb{S}$. Further, the collision laws $p_{kl;ij}(\mathbf{v}, \mathbf{w}, \mathbf{n})$ and $r_{kl;ij}(\mathbf{v}, \mathbf{w}, \mathbf{n})$ are given, positive measurable functions on $\mathcal{D}_{ij;kl} \times \mathbb{S}$. They are proportional to the probability of occurrence of reaction (1). Moreover,

$$p_{kl;ij}(\mathbf{v}, \mathbf{w}, \mathbf{n}) = p_{kl;ji}(\mathbf{w}, \mathbf{v}, \mathbf{n}) = p_{lk;ij}(\mathbf{v}, \mathbf{w}, -\mathbf{n}), \tag{12}$$

$$r_{kl;ij}(\mathbf{v}, \mathbf{w}, \mathbf{n}) = r_{kl;ji}(\mathbf{w}, \mathbf{v}, \mathbf{n}) = r_{lk;ij}(\mathbf{v}, \mathbf{w}, -\mathbf{n}), \tag{13}$$

$$\int_{\mathcal{D}_{ij;kl}\times\mathbb{S}} \varphi(\mathbf{v}, \mathbf{w})\, p_{kl;ij}(\mathbf{v}, \mathbf{w}, \mathbf{n})\, \psi(\mathbf{v}_{kl;ij}, \mathbf{w}_{kl;ij})\, d\mathbf{v}\, d\mathbf{w}\, d\mathbf{n}$$

$$= \int_{\mathcal{D}_{kl;ij}\times\mathbb{S}} \varphi(\mathbf{v}_{ij;kl}, \mathbf{w}_{ij;kl}), r_{ij;kl}(\mathbf{v}, \mathbf{w}, \mathbf{n})\, \psi(\mathbf{v}, \mathbf{w})\, d\mathbf{v}\, d\mathbf{w}\, d\mathbf{n}, \tag{14}$$

and

$$\int_{\mathcal{D}_{ij;kl}\times\mathbb{S}} \varphi(\mathbf{v},\mathbf{w})(\mathbf{v},\mathbf{w},\mathbf{n})\psi(\mathbf{v}_{kl;ij},\mathbf{w}_{kl;ij})\,d\mathbf{v}\,d\mathbf{w}\,d\mathbf{n}$$
$$= \int_{\mathcal{D}_{kl;ij}\times\mathbb{S}} \varphi(\mathbf{v}_{ij;kl},\mathbf{w}_{ij;kl})\psi(\mathbf{v},\mathbf{w})\,d\mathbf{v}\,d\mathbf{w}\,d\mathbf{n} \tag{15}$$

for all $(\varphi,\psi)\in C(\mathbb{R}^3\times\mathbb{R}^3)\times C_c(\mathbb{R}^3\times\mathbb{R}^3)\cup C_c(\mathbb{R}^3\times\mathbb{R}^3)\times C(\mathbb{R}^3\times\mathbb{R}^3)$. Here, as usual, $C(\mathbb{R}^3\times\mathbb{R}^3)$ denotes the space of real continuous functions on $\mathbb{R}^3\times\mathbb{R}^3$ and $C_c(\mathbb{R}^3\times\mathbb{R}^3)$ is the subspace of $C(\mathbb{R}^3\times\mathbb{R}^3)$ consisting of functions with compact support.

It is known [5] that, if $r_{ij;kl}(\mathbf{v},\mathbf{w},\mathbf{n})\le C(1+|\mathbf{v}|^2+|\mathbf{w}|^2)$ for some constant, $C>0$, then the Cauchy problem associated with the system (5) has, in some sense, unique positive global solutions $f_i(t)\in\mathbb{L}^1(\mathbb{R}^3;d\mathbf{v})-$ real, $1\le i\le N$, provided that the initial data are positive and their fourth-order momenta are well defined. In addition, the solutions satisfy the global mass, momentum, and energy (kinetic + internal) conservation (for more details the interested reader is referred to [5–7]).

For the numerical purposes of this paper, we apply the above considerations to a gaseous mixture composed of $N=4$ species. Only the following collisions (reactions) are supposed to govern the gas evolution:

(a) nonreactive collisions

$$X_i + X_j \to X_i + X_j, \tag{16}$$

whenever $1\le i,j\le 4$, unless $\{i,j\}\ne\{3,4\}$; and

(b) reactions of the form

$$X_1 + X_2 \to X_3 + X_4 \tag{17}$$

as well as the reverse reactions

$$X_3 + X_4 \to X_1 + X_2. \tag{18}$$

We suppose that reaction (17) is endothermic ($E_1+E_2<E_3+E_4$), so that reaction (18) is exothermic.

In the following, we need a weak form of Eq. (5), formulated for the above reactions, namely,

$$\left(\phi,\frac{\partial f_i}{\partial t}\right) = (\phi,P_i(\mathbf{f})) - (\phi,S_i(\mathbf{f})), \qquad (\forall)1\le i\le 4;\quad \phi\in C_b(\mathbb{R}^3), \tag{19}$$

where, by (14),

$$(\phi,P_i(\mathbf{f})) = \sum_{j,k,l=1}^{4}\int_{\mathcal{D}_{kl;ij}\times\mathbb{S}} \phi(\mathbf{v}_{ij;kl})\cdot r_{ij;kl}\cdot f_k(\mathbf{v})\,f_l(\mathbf{w})\,d\mathbf{v}\,d\mathbf{w}\,d\mathbf{n} \tag{20}$$

and

$$(\phi,S_i(\mathbf{f})) = \sum_{j,k,l=1}^{4}\int_{\mathcal{D}_{ij;kl}\times\mathbb{S}} \phi(\mathbf{v})\cdot r_{kl;ij}\cdot f_i(\mathbf{v})\,f_j(\mathbf{w})\,d\mathbf{v}\,d\mathbf{w}\,d\mathbf{n}. \tag{21}$$

Here $C_b(\mathbb{R}^3)$ denotes the space of continuous, bounded, real functions on $\mathbb{R}^3$.

According to the model, only the collision laws associated to reactions (16), (17), (18) may not vanish identically. For this reactions, we consider the following correspondents of the collision laws introduced by Krook and Wu for nonreactive gaseous mixtures [8].

ASSUMPTION.

$$r_{12;12}(\mathbf{v}, \mathbf{w}, \mathbf{n}) = \begin{cases} const \geq 0 & when\ \bar{W}_{12;34}(\mathbf{v}, \mathbf{w}, \mathbf{n}) < 0, \\ 0 & when\ \bar{W}_{12;34}(\mathbf{v}, \mathbf{w}, \mathbf{n}) \geq 0; \end{cases} \tag{22}$$

the functions $r_{12;34}, r_{34;12}$ are nonnegative constants (*on their domains*); *similarly $r_{ij;ij}$ is nonnegative and constant if $\{i, j\} \neq \{1, 2\}$ or $\{i, j\} \neq \{3, 4\}$.*

By (14) we also put $p_{kl;ij}(\mathbf{v}, \mathbf{w}, \mathbf{n}) = r_{ij;kl}(\mathbf{v}_{kl;ij}(\mathbf{v}, \mathbf{w}, \mathbf{n}), \mathbf{w}_{kl;ij}(\mathbf{v}, \mathbf{w}, \mathbf{n}), \mathbf{n})$.

Obviously, the present model is isotropic; i.e., $f_i(\mathbf{v}) = f_i(v)$ for $1 \leq i \leq 4$ (where $v := |\mathbf{v}|$ is the modulus of the velocity $\mathbf{v}$). The above assumption allows us to provide a more explicit form for Eq. (19). To this end, we consider the new unknowns

$$F_i(v) := 4\pi v^2 f_i(v), \quad \text{for } 1 \leq i \leq 4, \tag{23}$$

and we denote the concentration of the species i by

$$I_i := \int_0^\infty F_i(v)\, dv, \quad \text{for } 1 \leq i \leq 4. \tag{24}$$

Introducing the notation $\lambda_{kl;ij} := 4\pi r_{ij;kl}$ $(1 \leq i, j, k, l \leq 4)$ and using suitable changes of variables in (20) and (21), these formulae become

$$(\phi, P_i(\mathbf{f})) = \sum_{j,k,l=1}^{4} \lambda_{kl;ij} \cdot I_k I_l \int_{\mathbb{D}_{kl;ij}} \phi(\tilde{v}) \cdot F_k(v) F_l(w)\, dv\, dw\, d\zeta\, d\eta, \tag{25}$$

$$(\phi, S_i(\mathbf{f})) = \sum_{j,k,l=1}^{4} \lambda_{ij;kl} \cdot I_i I_j \int_{\mathbb{D}_{ij;kl}} \phi(v) \cdot F_i(v) F_j(w)\, dv\, dw\, d\zeta\, d\eta, \tag{26}$$

where

$$\mathbb{D}_{kl;ij} := \{(v, w, \zeta, \eta) \in \mathbb{R}_+^2 \times [0, 1)^2 \mid \tilde{v}_{kl;ij} \in \mathbb{R}\} \tag{27}$$

and $\tilde{v}_{kl;ij}$ (the postcollision velocity of the species i) is given by

$$\tilde{v}_{kl;ij} = \tilde{v}_{kl;ij}(v, w, \zeta, \eta) := \left[V_{kl}^2 + \frac{m_k}{m_l} \rho_{kl;ij}^2 + 2 \left(\frac{m_k}{m_l} \right)^{1/2} \rho_{kl;ij} V_{kl} (2\eta - 1) \right]^{1/2}, \tag{28}$$

with

$$V_{kl} = V_{kl}(v, w, \zeta) := \left(m_k^2 v^2 + m_l^2 w^2 + 2 m_k m_l v w (2\zeta - 1) \right)^{1/2} / (m_k + m_l), \tag{29}$$

$$\rho_{kl;ij} = \rho_{kl;ij}(v, w, \zeta) := [m_k m_l (v^2 + w^2 + 2vw(2\zeta - 1))/(m_k + m_l)^2 + 2(E_k + E_l - E_i - E_j)(m_k + m_l)]^{1/2}. \tag{30}$$

As mentioned in Section 1, one does not know nontrivial solutions of Eq. (19) with the P_i and S_i given by (25) and (26). Therefore, numerical tests on exact solutions are not yet

possible. However, indirect tests can be performed, because, starting from (19), (25), and (26), one can solve exactly the equations for chemical concentrations. Specifically, suppose that particles of species X_1 and X_2 interact only by elastic collisions. Then, one finds easily that

$$\begin{cases} \dot{I}_i = \lambda \cdot I_3 I_4, & i = 1, 2, \\ \dot{I}_i = -\lambda \cdot I_3 I_4, & i = 3, 4, \end{cases} \tag{31}$$

where $\lambda := \lambda_{34;12}$.

Denote $I_i^0 := I_i(0)$, $1 \le i \le 4$. We distinguish two situations:

1. If $I_3^0 \neq I_4^0$, then the solutions of (31) are

$$\begin{cases} I_i(t) = I_i^0 + \frac{I_3^0 I_4^0 \cdot [\exp(I_4^0 \cdot \lambda t) - \exp(I_3^0 \cdot \lambda t)]}{I_4^0 \cdot \exp(I_4^0 \cdot \lambda t) - I_3^0 \cdot \exp(I_3^0 \cdot \lambda t)}, & i = 1, 2, \\ I_i(t) = \frac{I_i^0 (I_4^0 - I_3^0) \cdot \exp(I_i^0 \cdot \lambda t)}{I_4^0 \cdot \exp(I_4^0 \cdot \lambda t) - I_3^0 \cdot \exp(I_3^0 \cdot \lambda t)}, & i = 3, 4. \end{cases} \tag{32}$$

2. If $I_3^0 = I_4^0$, then

$$\begin{cases} I_i(t) = I_i^0 + \frac{(I_3^0)^2 \cdot \lambda t}{(1 + I_3^0 \cdot \lambda t)}, & i = 1, 2, \\ I_i(t) = \frac{I_i^0}{(1 + I_i^0 \cdot \lambda t)}, & i = 3, 4. \end{cases} \tag{33}$$

Now we can obtain exact expressions for energies. Indeed, the contribution to the gas energy due to the internal energy of the particles is

$$E_{int}(t) = \sum_{i=1}^{4} I_i(t) E_i. \tag{34}$$

Then, by virtue of the global conservation of energy, the total (kinetic + internal) energy of the gas particles is

$$E(t) = \sum_{i=1}^{4} \frac{m_i \langle v_i^2 \rangle(t)}{2} + \sum_{i=1}^{4} I_i(t) E_i = E(0). \tag{35}$$

Also, the total kinetic energy of the particles is given by the formula

$$E_{cin}(t) = \sum_{i=1}^{4} \frac{m_i \langle v_i^2 \rangle(t)}{2} = \sum_{i=1}^{4} \frac{m_i \langle v_i^2 \rangle(0)}{2} + \sum_{i=1} \left[I_i^0 - I_i(t) \right] E_i. \tag{36}$$

Under the above considerations, one can compare the exact values of concentrations and energies with those computed by means of the distribution functions resulting from the numerical solution of the system (19), (25), and (26) by the method of [7]. Moreover, one can check the conservation of concentrations and global energy for the aforementioned numerical solutions.

3. NUMERICAL METHOD

In this section we show how the particle method of [7] can be applied to obtain numerical solutions of the Cauchy problem for Eq. (19). The procedure requires several steps:

STEP I. *For a sufficiently small time step, one introduces a time-discretized version of Eq.* (19) *and provides a convergent iteration scheme for solutions.*

STEP II. *One approximates the initial data by weakly convergent sums of Dirac measures.*

STEP III. *The iteration scheme produces a weakly convergent sequence of approximating solutions, indexed by the iteration order. Every approximating solution is also the sum of Dirac measures. However, because of the nonlinearity, each iteration step produces a power-like growing number of terms in the sums of point measures. In computations, the numerical effort would also have a power-like increase, so that the algorithm could not be effective, at this level. This is the moment when the stochastic element is introduced*: *one limits the number of terms of the Dirac sums, by random selection. Then, according to the central result in* [7] (*Theorem* 10), *it follows that, the numerical solutions almost always converge weakly* (*in the sense of measures*) *to the exact solutions of the equations.*

Specifically, we proceed as follows:

Step I. To write the time-discretized equations, we first introduce some new notation. For $\{i, j\} = \{1, 2\}$ and $\{k, l\} = \{3, 4\}$ define the measures

$$\begin{aligned} d\bar{H}_{ij}(v, w, \zeta, \eta) &:= \frac{1}{J_{ij}} F_i(v)F_j(w)\, dv\, dw\, d\zeta\, d\eta \qquad \text{on } \mathbb{D}_{ij;kl}, \\ d\underline{H}_{ij}(v, w, \zeta, \eta) &:= \frac{1}{\underline{J}_{ij}} F_i(v)F_j(w)\, dv\, dw\, d\zeta\, d\eta \qquad \text{on } \mathbb{R}^2_+ \times [0, 1]^2 \backslash \mathbb{D}_{ij;kl}, \end{aligned} \tag{37}$$

where

$$\begin{aligned} \bar{J}_{ij} &:= \int_{\mathbb{D}_{ij;kl}} F_i(v)F_j(w)\, dv\, dw\; d\zeta\, d\eta, \\ \underline{J}_{ij} &:= \int_{\mathbb{R}^2_+ \times [0,1]^2 \backslash \mathbb{D}_{ij;kl}} F_i(v)F_j(w)\, dv\, dw\, d\zeta\, d\eta\,. \end{aligned} \tag{38}$$

For $\{i, j\} = \{1, 2\}$, define the measure

$$dH_{ij}(v, w, \zeta, \eta) := \frac{1}{I_i I_j} F_i(v)F_j(w)\, dv\, dw\, d\zeta\, d\eta \qquad \text{on } \mathbb{R}^2_+ \times [0, 1)^2. \tag{39}$$

Let $[[x]]$ denote the integer part of the real positive number x. Consider some time interval $[0, T]$ and some given time step $0 < \Delta t < T$. Then the discretized equations associated with (19) with initial data $F_i^0(v)$, $1 \le i \le 4$ has the form

$$\left(\phi, F_i^{p+1}\right) = \left(\phi, Q_{ij}^p\right), \tag{40}$$

where $\{i, j\} = \{1, 2\}$ or $\{i, j\} = \{3, 4\}$, $p \in \{0, 1, \ldots, J-1\}$, $J := [[T/\Delta t]]$, and $\phi \in C_b(\mathbb{R})$. Here Q_{ij}^p is defined as follows:

if $\{i, j\} = \{1, 2\}$, then

$$\begin{aligned}(\phi, Q_{ij}^p) := &\left[\sum_{k=1}^4 \left(\frac{m_k}{M_{tot}^p} - \lambda_{ik;ik}\Delta t\right) I_k^p - \lambda_{ii;ii}\Delta t I_i^p\right] I_i^p (\phi, F_i^p) \\ &+ \left[\left(\frac{m_j}{M_{tot}^p} - \lambda_{ij;ij}\Delta t\right)\underline{J}_{ij}^p(\phi, \underline{H}_{ij}^p) + \left(\frac{m_j}{M_{tot}^p} - \lambda_{ij;34}\Delta t\right)\bar{J}_{ij}^p(\phi, \bar{H}_{ij}^p)\right] I_j^p I_i^p \\ &+ \left[\lambda_{ii;ii}(\tilde{\phi}_{ii;ii}, H_{ii}^p) I_i^p + \sum_{k=1}^4 \lambda_{ik;ik}(\tilde{\phi}_{ik;ik}, H_{ik}^p) I_k^p\right]\Delta t I_i^p \\ &+ \left[\lambda_{ij;ij}\underline{J}_{ij}^p(\tilde{\phi}_{ij;ij}, \underline{H}_{ij}^p) I_j^p I_i^p + \lambda_{34;ij}(\tilde{\phi}_{34;ij}, H_{34}^p) I_3^p I_4^p\right]\Delta t; \end{aligned} \tag{41}$$

if $\{i, j\} = \{3, 4\}$, then

$$\begin{aligned}(\phi, Q_{ij}^p) := &\left[\sum_{k=1}^4 \left(\frac{m_k}{M_{tot}^p} - \lambda_{ik;ik}\Delta t\right) I_k^p - \lambda_{ii;ii}\Delta t I_i^p\right] I_i^p (\phi, F_i^p) \\ &+ \left[\lambda_{ii;ii}(\tilde{\phi}_{ii;ii}, H_{ii}^p) I_i^p + \sum_{k=1}^4 \lambda_{ik;ik}(\tilde{\phi}_{ik;ik}, H_{ik}^p)\, I_k^p\right]\Delta t I_i^p \\ &+ \lambda_{12;ij}\bar{J}_{12}^p(\tilde{\phi}_{12;ij}, \bar{H}_{12}^p)\Delta t I_1^p I_2^p. \end{aligned} \tag{42}$$

In (41) and (42) the quantities I_i^p, $\underline{H}_{ij}^p$, $\bar{H}_{ij}^p$, $\underline{J}_{ij}^p$, $\bar{J}_{ij}^p$, and H_{ij}^p are defined as in (24), (37), (38), and (39), simply by replacing F_i and F_j by F_i^p and F_j^p respectively. Moreover,

$$M_{tot}^p := \sum_{i=1}^4 m_i I_i^p \tag{43}$$

and $\tilde{\phi}_{ij;kl} := \phi \circ \tilde{v}_{ij;kl}$, with $\tilde{v}_{ij;kl}$ given by (28).

An inspection of the above formulas shows that (40) takes the useful form as equation for measures

$$\begin{aligned}(\phi, \nu_i^{p+1}) = (\phi, \nu_i^p) &- \Delta t \sum_{j,k,l=1}^4 \lambda_{ij,kl} \int_{\mathbb{D}_{ij,kl}} \phi(v)\, d\nu_i^p(v)\, d\nu_j^p(w)\, d\zeta\, d\eta \\ &+ \Delta t \sum_{j,k,l=1}^4 \lambda_{kl,ij} \int_{\mathbb{D}_{kl,ij}} \tilde{\phi}_{kl,ij}(v)\, d\nu_k^p(v)\, d\nu_l^p(w)\, d\zeta\, d\eta, \end{aligned} \tag{44}$$

where $d\nu_i^p(v) := F_i^p(v)\, dv$ $1 \le i \le 4$, $p \in \{0, 1, \ldots, J-1\}$.

Step II. According to the scheme of [7], we approximate ν_i^0 by convergent sequences of discrete measures of the form

$$\mu_n^0 = \frac{a_n}{n} \sum_{p=1}^n \delta_{v_p^0}, \tag{45}$$

with $a_n > 0$ depending on initial mass densities and where $\delta_{v_p^0}$ denotes the Dirac measure

concentrated on v_p^0. We also approximate the Lebesgue measure on the unit square $d\zeta d\eta$ by sums of Dirac measures of the form $\frac{1}{n}\sum_{p=1}^{n}\delta_{\zeta_p}\delta_{\eta_p}$.

One possible way to provide this kind of approximations is to use low-discrepancy methods which minimize the discrepancy [9]. Here we recall that the discrepancy $D(\mu,\mu')$ of the real measures μ and μ' on $\mathbb{R}^q$ is defined by

$$D(\mu,\mu') := \sup_{a\in\mathbb{R}^q}\left|\int_{X_a} d\mu - \int_{X_a} d\mu'\right|, \tag{46}$$

where $X_a := \{(x_1,\dots,x_q)\in\mathbb{R}^q \mid x_i \le a_i, 1\le i\le q\}$, with $a := (a_1,\dots,a_q)$.

Step III. Because of the product measures in the right-hand-side of (44), for a given input Dirac sum of n terms, the next iteration step yields a sum of Dirac measures concentrated on $n+cn^3$ points (with c a natural constant). This implies a power-like increasing computational effort. To decrease the computational effort and preserve the convergence of the scheme, one appeals to random selection by applying Theorems 7 and 8 of [7].

Therefore, giving for chemical species $1\le i\le 4$, an initial datum, say $\nu_i^{0,0}$ of the form (45), the algorithm follows the computational chain $\nu_i^{0,0}\to\nu_i^{1,1}\to\nu_i^{2,2}\to\cdots\to\nu_i^{J-1,J-1}\to\nu_i^{J,J}$ corresponding to the diagonal of the scheme

$$\begin{array}{ccccccccc}
\nu_i^{0,0} & \to & \nu_i^{0,1} & \to & \nu_i^{0,2} & \to\cdots\to & \nu_i^{0,J-1} & \to & \nu_i^{0,J}\\
 & & \wr\wr & & & & & & \\
 & & \nu_i^{1,1} & \to & \nu_i^{1,2} & \to\cdots\to & \nu_i^{1,J-1} & \to & \nu_i^{1,J}\\
 & & & & \wr\wr & & & & \\
 & & & & \nu_i^{2,2} & \to\cdots\to & \nu_i^{2,J-1} & \to & \nu_i^{2,J}\\
 & & & & & & \vdots & & \vdots\\
 & & & & & & \wr\wr & & \\
 & & & & & & \nu_i^{J-1,J-1} & \to & \nu_i^{J-1,J}\\
 & & & & & & & & \wr\wr\\
 & & & & & & & & \nu_i^{J,J}.
\end{array} \tag{47}$$

Here, the horizontal chains represent the exact iterations of the time-discretized equations, such that for each $0\le k\le J-1$ and $k+1\le p\le J$ the measure $\nu_i^{k,p}$ is given as the $(p-k)$th iteration for the input data $\nu_i^{k,k}$. In addition, $\nu_i^{k,k}$, $1\le k\le J$, is provided by the random selection form $\nu_i^{k-1,k}$, $k\ge 1$.

The weighted random selection method used in this paper increases the efficiency of the method, compared to the uniform selection procedure used in [7, 13]. More specifically, instead of associating (at every time step) the same number of concentration points with each one-particle distribution function, we choose the number of concentration points "proportional" to the physical concentration of the species. We fix a number n and approximate ν_i^0 by sums of the form (45) concentrated on $n_i^0 = [[n\cdot I_i^0/\sum_{j=1}^4 I_j^0]]$ points. At iteration step p, we select a number $n_i^p = [[n\cdot I_i^p/\sum_{j=1}^4 I_j^p]]$ of concentration points, for each species i.

Finally we recall the idea behind the selection rule of [7]. Consider the probability space (Ω,β_Ω,P), with $\Omega=[0,1)^\infty$ (in countable sese), β_Ω the standard σ-algebra of Borel subsets of Ω, and P the measure of probability induced by uniform distribution on $[0,1)$.

Let μ be a discrete measure concentrated on $V = \{v_1, v_2, \ldots, v_m\} \subset \mathbb{R}^q$,

$$\mu = \mu_m = \frac{1}{m} \sum_{i=1}^{m} \delta_{v_i}. \tag{48}$$

We are interested in approximating (48) by a sum of the same form with $n = n(m) \leq m$ terms. For $1 \leq k \leq n$ consider the random variables $i_k : \Omega \to \{1, 2, \ldots, m\}$,

$$i_k(\omega) := [[\omega_k \cdot m]] + 1. \tag{49}$$

Then $i_1, \ldots, i_n$ select randomly n terms of the sum in (48). Defining

$$\nu = \nu_n := \frac{1}{n} \sum_{k=1}^{n} \delta_{v_{i_k(\omega)}}, \tag{50}$$

We can show that if μ_m converges weakly as $m \to \infty$, then for almost all $\omega \in \Omega$, the sum (50) converges to the same limit, as $n \to \infty$ (for more details see [7]).

4. NUMERICAL RESULTS

Our experiments consisted of several tests of the model introduced in Section 2, applied to three and four distinct gaseous species with binary chemical reactions. The analysis provides oversimplified characterizations of the following examples of dilute reacting fluids:

—mixture of N_2, O_2, and NO with reaction $N_2 + O_2 \to 2NO$,
—mixture of HF, HCl, FCl, and F_2 with reaction $HF + FCl \to F_2 + HCl$,
—mixture of BrF, FCl, BrCl, and F_2 with reaction $F_2 + BrCl \leftrightarrow BrF + FCl$.

Since the numerical experiments on the models with three and four components lead to similar results, our presentation will refer only to a gas model with four interacting species.

In this respect, we considered the following three situations:

Case 1: Four distinct species with nonreactive collisions and exothermic reactions of the form $HF + FCl \to F_2 + HCl$ in gaseous mixtures of HF, HCl, FCl, and F_2 at sufficiently low temperatures (only processes (16), and (18) occur and $X_1, \ldots, X_4$ are different).

In this case the model has exact solutions for concentrations and kinetic and internal energies (32), (36), and (34), respectively.

Although the numerical scheme is nontrivially applied to this case, the absence of endothermic reaction leads to a simplification because, by threshold considerations, $\underline{J}_{ij} = 1$ and $\bar{J}_{ij} = 0$ in (38). Then the information provided by the results of Case 1 might not be sufficiently relevant to describe the gas with both exothermic and endothermic reactions. Therefore we considered a separate situation:

Case 2: Four distinct species, e.g., nonreactive collisions, endothermic and exothermic reactions of the form $BrF + FCl \to F_2 + BrCl$, and $F_2 + BrCl \to BrF + FCl$, in gaseous mixtures of BrF, FCl, BrCl, and F_2 (all processes (16), (17), and (18) occur and $X_1, \ldots, X_4$ are different).

Unfortunately, in this situation, we do not know exact solutions of the equations for macroscopic quantities. However, the results obtained are still useful since they provide qualitative information on the time behavior of the macroscopic variables and enable a nontrivial check of the conservation laws.

To test the method when the thermodynamic quantities are oscillating in time, we considered the following modification of Case 1 by adding an exterior pulsating source.

Case 3: The model of Case 1 with a pulsating external source of particles—a simplified description of the homogeneous combustion, with injection and evacuation.

Specifically, we solved numerically Eqs. (5) with a source term of the form

$$\sigma_i := g_i \cdot \sum_{l=1}^{\infty} \delta(t - l \cdot \tau) - 2p \Bigg/ \left(2p + \sum_{k=1}^{4} \int_{\mathbb{R}^3} f_k \, d\mathbf{v} \right) \cdot f_i \cdot \sum_{l=1}^{\infty} \delta(t - \tau_0 - l \cdot \tau), \quad (51)$$

for $i = 1, 2, 3, 4$. Here $g_i := 0$, for $i = 1, 2$; $g_i = g_i(\mathbf{v}) := p \cdot f_i(0, \mathbf{v})$, for $i = 3, 4$; and p is a positive constant.

As in Case 1, this model also has exact solutions which can be easily deduced iteratively from (32), (34), and (36).

Here it should be emphasized that the numerical method can be applied to models with more complicated source terms added to Eqs. (5) (e.g., represented by functions that can be approximated by weighted sums of Dirac distributions).

We used the following input data (expressed in conventional, dimensionless units):

Case 1:

Masses: $m_1 = 33.20 \times 10^{-7}$, $m_2 = 90.47 \times 10^{-7}$, $m_3 = m_4 = 63.08 \times 10^{-7}$.

Initial concentrations: $I_1^0 = 0.02$, $I_2^0 = 0.08$, $I_3^0 = 0.4$, $I_4^0 = 0.5$.

Internal energies: $E_1 = -42.4750$, $E_2 = 9.3264$, $E_3 = 24.7642$, $E_4 = -20.7251$.

Values of λ: $\lambda_{11;11} = 1.2582$, $\lambda_{12;12} = \lambda_{34;12} = 2.1073$, $\lambda_{12;34} = 0$, $\lambda_{13;13} = 1.6091$, $\lambda_{14;14} = 1.7564$, $\lambda_{22;22} = 2.9564$, $\lambda_{23;23} = 2.4582$, $\lambda_{24;24} = 2.6055$, $\lambda_{33;33} = 1.9600$, $\lambda_{44;44} = 2.2547$.

Initialization time $t = 0$; final time $T = 8.5$.

Initialization function in the time-discretized equations:

$$F_i^0(v) = 4\pi v^2 I_i^0 \left(\frac{m_i}{\pi} \right)^{3/2} \exp(-m_i v^2), \quad 1 \le i \le 4. \quad (52)$$

Case 2:

Masses: $m_1 = 164.34 \times 10^{-7}$, $m_2 = 90.47 \times 10^{-7}$, $m_3 = 63.08 \times 10^{-7}$, $m_4 = 191.73 \times 10^{-7}$.

Initial concentrations: $I_1^0 = 0.35$, $I_2^0 = 0.6$, $I_3^0 = 0.05$, $I_4^0 = 0$.

Internal energies: $E_1 = -15.3415$, $E_2 = -15.6736$, $E_3 = -0.2328$, $E_4 = -10.1946$.

Values of λ: $\lambda_{11;11} = 3.6020$, $\lambda_{12;12} = \lambda_{34;12} = 3.2792$, $\lambda_{12;34} = 3.2792$, $\lambda_{13;13} = 2.7810$, $\lambda_{14;14} = 4.1002$, $\lambda_{22;22} = 2.9564$, $\lambda_{23;23} = 2.4582$, $\lambda_{24;24} = 3.7774$, $\lambda_{33;33} = 1.9600$, $\lambda_{44;44} = 4.5985$.

Initialization time $t = 0$; final time $T = 1.75$.

Initialization function in the time-discretized equations:

$$F_i^0(v) = 4\pi v^2 I_i^0 \left(\frac{m_i}{20\pi} \right)^{3/2} \exp\left(-\frac{m_i v^2}{20} \right), \quad 1 \le i \le 4. \quad (53)$$

Case 3:

We use the same data as in Case 1; in addition, $p = 0.2$, $\tau = 2$, and $\tau_0 = 1$, for the source term (51).

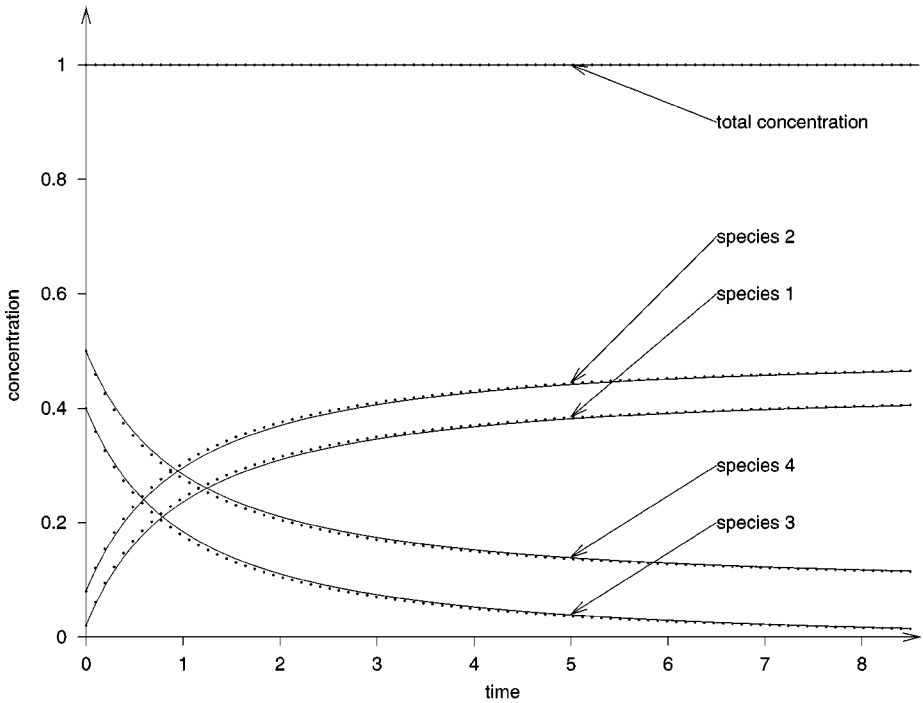

FIG. 1. The evolution of the concentrations in Case 1 for 88 iteration steps.

The approximation of the initial data by low-discrepancy sums of Dirac measures was made by means of the Hammersley–Van der Corput sequences (see [9]). The "support" of F_i^0 was included in [0, 2000] and [0, 6000] for F_i^0 given by (52) and (53), respectively.

We used the mixed congruential method to generate sequences of pseudo-random numbers $\{\omega_n\}_{n\in\mathbb{N}}$. The elements $\omega_n = z_n/b$, where z_n are given recursively by $z_n = \lambda z_{n-1} + r \pmod{b}$. In this relation, $b > 1$, λ and r are fixed natural numbers, and λ is relatively prime to b. The initialization is made with some integer $0 \le z_0 < b$. Here $b = 3 \times 10^{30}$, $r = 1987654321$, and $\lambda = 19867917$. Each test starts with an arbitrary positive $z_0 < b$.

Our results are summarized in Figs. 1–6, presenting the evolution of the concentrations and energies for 88 iteration steps in Case 1, 44 iteration steps in Case 2, and 150 iteration steps in Case 3. The results provided by the numerical method are indicated by dots. Each dot corresponds to a number given by the arithmetic mean of the values obtained as results of m simulations (corresponding to identical physical conditions). We set $m = 6$ in Cases 1 and 2 and $m = 15$ in Case 3. In addition, we represent by continuous lines the values of the known exact solutions of the equations for the above macroscopic quantities. Here, we remark that due to the similarities in the behavior of concentrations in Case 3, we illustrate only the evolution of the concentration for species 1 (see Fig. 5), as a typical example.

Moreover, Figs. 2 and 4 detail the values of the kinetic energy, calculated by two different methods. Specifically, the first method evaluates the kinetic energy (kinetic energy 1, represented in our figures by circles) at each iteration step, as a difference between the total energy (at $t = 0$) and the numerical value of internal energy (expressed in terms of concentrations as in (36)). The second method yields the kinetic energy (kinetic energy 2, represented in our figures by points) as an average with respect to the one-particle distribution functions.

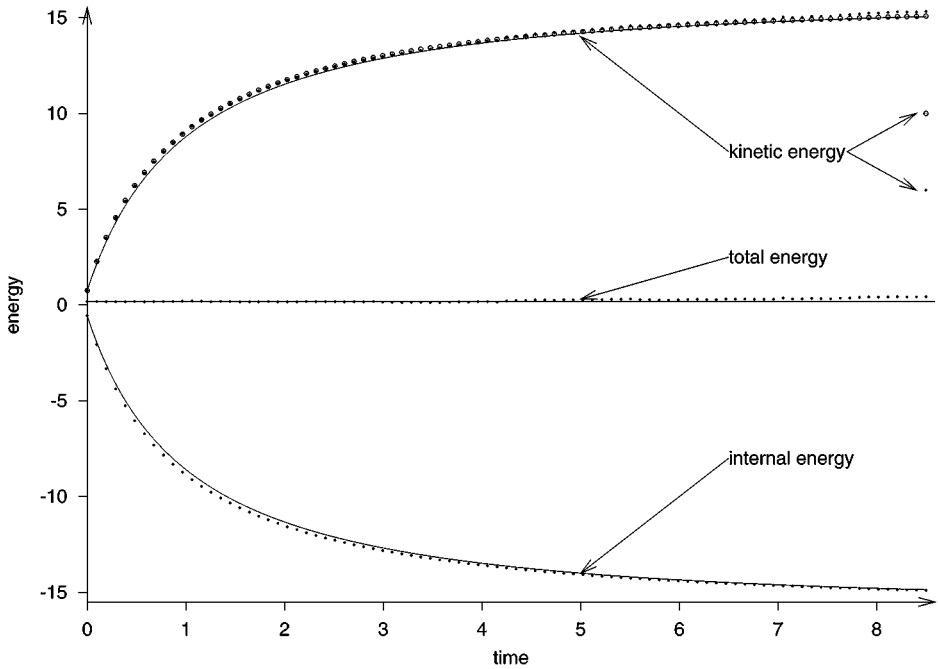

FIG. 2. The evolution of the energies in Case 1 for 88 iteration steps.

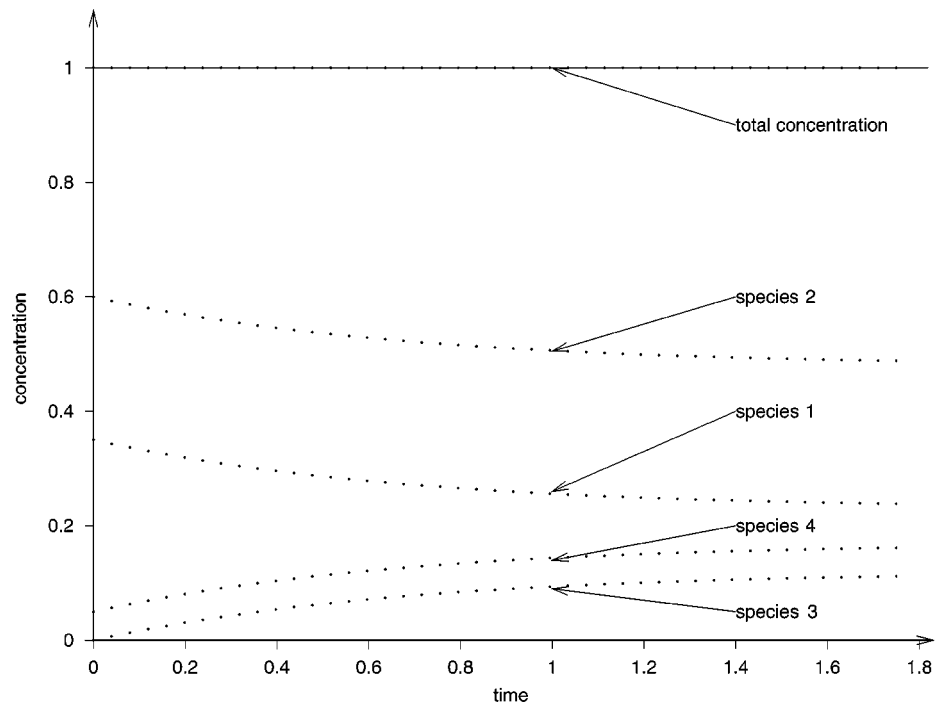

FIG. 3. The evolution of the concentrations in Case 2 for 44 iteration steps.

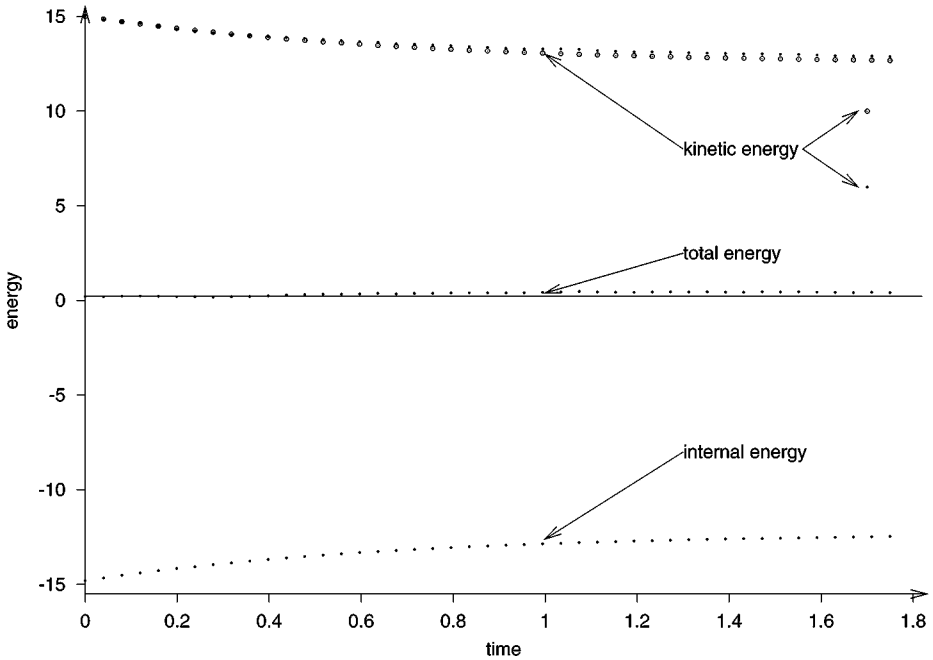

FIG. 4. The evolution of the energies in Case 2 for 44 iteration steps.

The results show good agreement between numerical and exact values.

With respect to the accuracy of the computations, one should observe that the derivation of the method introduces three basic sources of errors, which are due to the approximation of the initial data, to time discretization, and to stochastic selection, respectively.

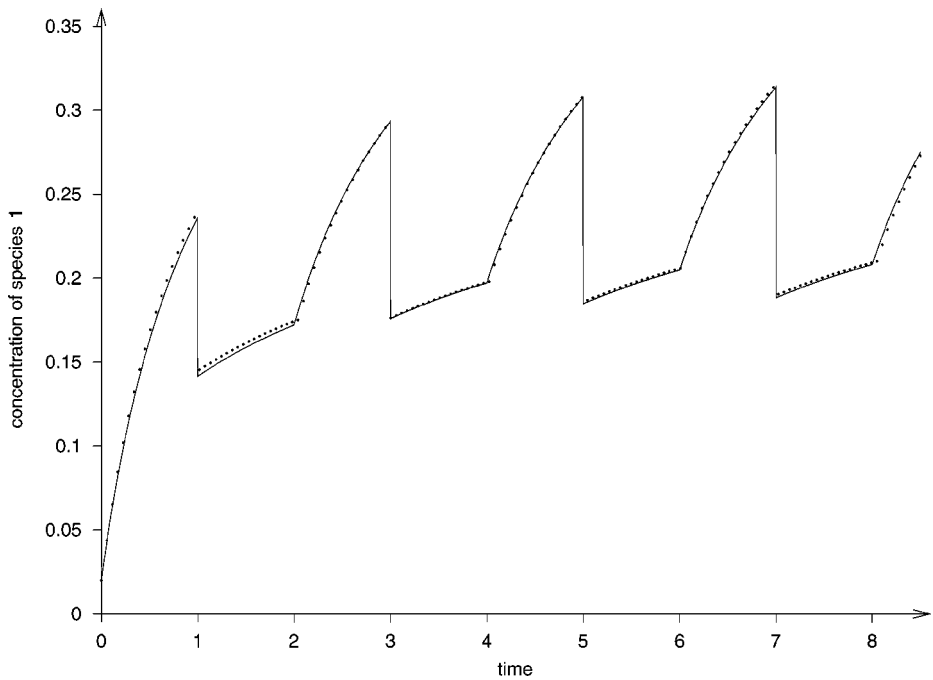

FIG. 5. The evolution of the concentration of species 1 in Case 3 for 150 iteration steps.

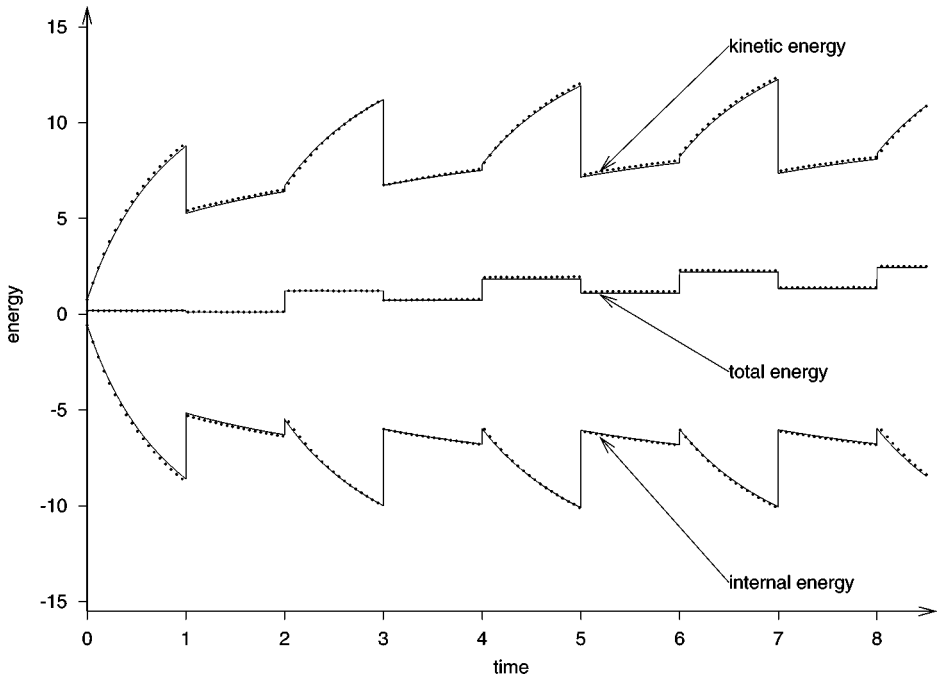

FIG. 6. The evolution of the energies in Case 3 for 150 iteration steps.

As is known [9], the approximation of the initial data by low discrepancy can be accurately controlled with little computational effort. However, the role of the errors introduced by time discretization and selections requires a more careful analysis, as illustrated by the following considerations.

Our first remark is that, in Case 1, in the calculation of the concentrations and internal energy, the stochastic selection was not needed. Consequently, the dominant contribution to errors came essentially from time discretization.

Further, it can be easily seen that, for an arbitrary (fixed) small enough time step, both the (autonomous) continuous and discrete dynamical systems associated with the evolution of the concentrations in Case 1 have the same attractor, namely, the point $(I_1^0 + I_3^0, I_2^0 + I_3^0, 0, I_4^0 - I_3^0)$, provided that $I_3^0 < I_4^0$. Consequently, in this case, the errors of the concentration have to decrease at large scale times. Moreover, the error of the internal energy has the same large time behavior, since the computation of the internal energy depends only on concentrations.

However, this behavior might be different in Case 3, where the continuous and discretized dynamical systems are not autonomous and one expects limit cycles. Here, obviously the time steps must be chosen sufficiently small with respect to the expected oscillation time scales.

Furthermore, the above errors in concentrations affect the computation of the distribution functions and, implicitly, the determination of the kinetic and total energies. On the other hand, in Case 1, the calculation of the last two quantities involves stochastic selection. However, for a reasonable computational effort, as in Case 1, we still expect the errors from time discretization to play a dominant role at small time scale. This is because after a small number of iterations/selection steps the errors accumulated by selection are still small compared with those due to discretization.

These phenomena are illustrated by Figs. 2 and 4.

We expect the same behavior of errors in the case when endothermic reactions are included in the model (Case 2). The main reason is that the discretization and selection procedures are essentially performed as in Case 1. Unfortunately, one cannot develop a similar argument as before, because, at least at our present level of understanding, one cannot compare the large-time behavior of the solutions of the continuous and discretized dynamical systems for concentrations as for Case 1.

Moreover, Fig. 2 shows the increase in the errors of kinetic and total energies at large time scale. This can be understood as the result of the accumulation of selection errors as time increases, and the same argument holds in Case 2. The accumulation of errors explains why in Fig. 2, for large time, "kinetic energy 1," calculated from concentrations (without selection) is closer to the exact values, than "kinetic energy 2" (which is computed directly from the distribution functions). The error accumulation also explains the difference, in Case 2, between the values of "kinetic energy 2" and "kinetic energy 1." Here these quantities are calculated as in Case 1 except that the random selection is also used to estimate integrals (38). Thus, in Case 2, "kinetic energy 1" is expected to provide more accurate values than "kinetic energy 2."

One can easily estimate the contribution of the stochastic errors using the standard deviation. However, we recall that the solution of the numerical scheme for the Boltzmann model results, after the time discretization of the model, by applying random selections to the solutions of the discretized system of equations. Therefore, in general the standard deviation measures only the errors of the solution of the numerical scheme with respect to that of the discretized system.

As was argued before, the behavior of the errors introduced by the stochastic part of the numerical method can be better illustrated on the case of energy. In this respect, we studied the evolution of the standard deviation and its dependence on the number of simulations, for the kinetic energy in Case 1 and for the total energy in Cases 1 and 2. For exemplification we present the results for the total energy in Case 2 (other situations are similar). Figure 7 illustrates the typical evolution of the stochastic errors and standard deviation with 6 and 40 tests.

In the particular Cases 1 and 2, the time discretization does not introduces any error in the computation of the total energy. Then the standard deviation also measures the total error in the evaluation of the total energy. The data in the graphics show that errors of the simulations are larger than the graphics scale.

The accumulation of the probabilistic errors can be also be noted in Fig. 7 by the tendency of the standard deviation to increase with time (for a fixed number of simulations).

However, because of the convergence, there is a tendency for an increase in the number of simulations to diminish the standard deviation. In this respect, Figs. 8 and 9 represent the dependence of the standard deviation on the number of tests for the total energy in Cases 1 and 2 at final time T. For a better illustration we also represent, in the same figures, the values of the error of the total energy for each test, as well as the dependence of the mean error in the total energy with respect to the number of tests. It also appears that the data presented in Figs. 2 and 4 (provided by a series of six simulations) correspond to a bigger error zone, and a reasonable increase of the number of simulations can diminish considerably the stochastic errors.

Therefore, by the convergence of the method, for a sufficiently large number of simulations the mean values of the calculated macroscopic quantities tend to stabilize at a value essentially determined by the time step of the discretization.

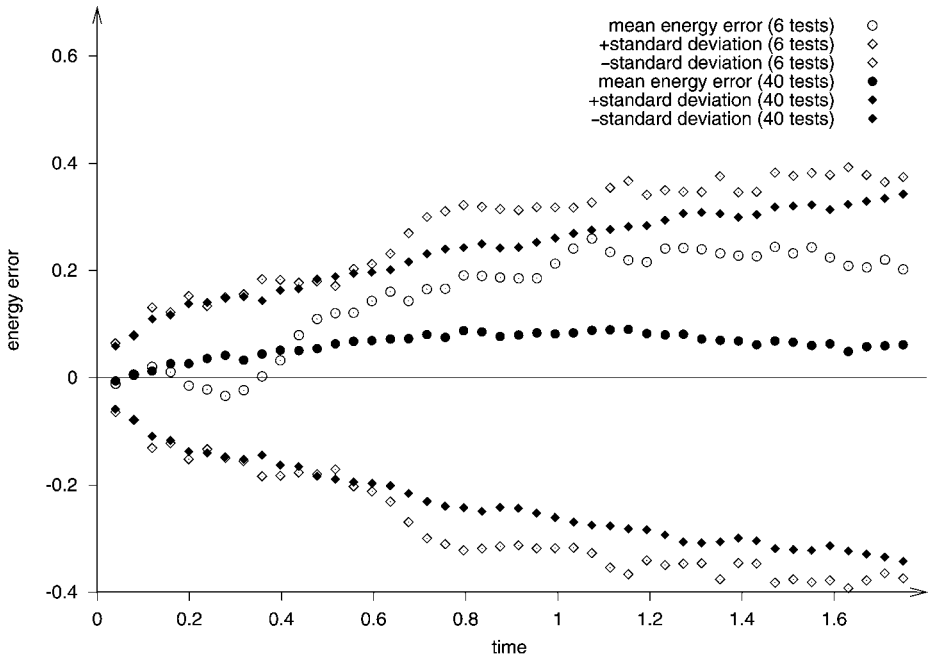

FIG. 7. Errors of total energy in Case 2 along 44 iteration steps.

On the other hand, it is known (Proposition 4 in [7]) that, in the absence of selections, the errors due to discretization can be improved by decreasing the time step. However, in the case of random selection (for a fixed number of concentration points), a decrease in time step does not necessarily result in a decrease of errors. This is because when the time

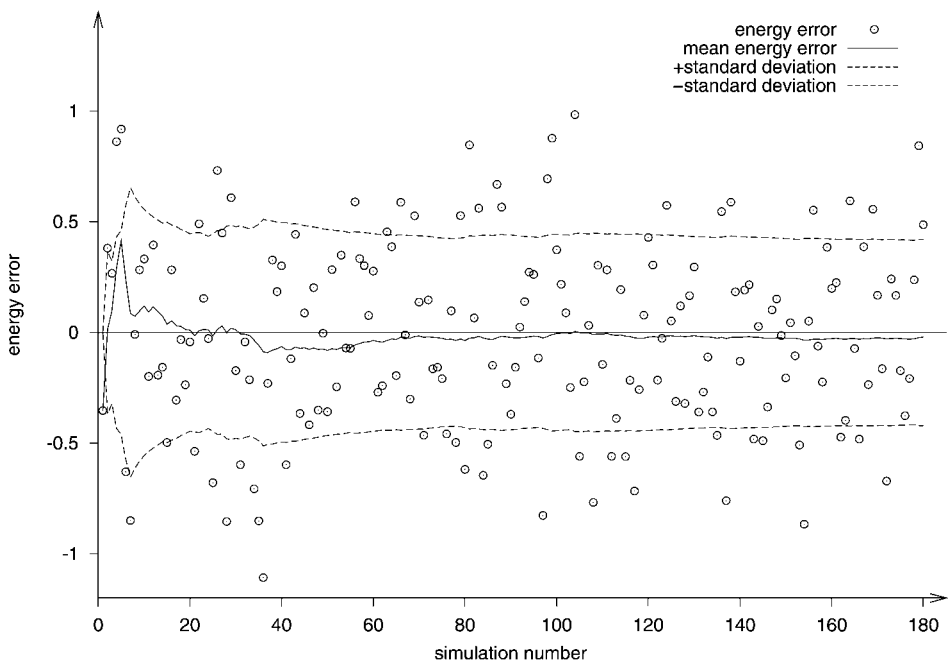

FIG. 8. Errors of total energy in Case 1 after 88 iteration steps.

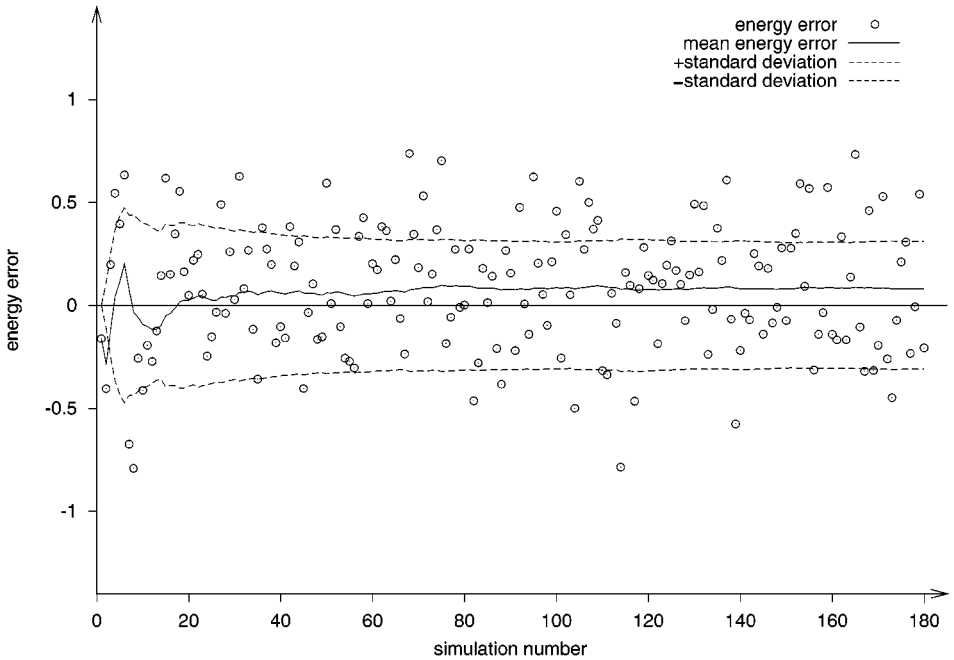

FIG. 9. Errors of total energy in Case 2 after 88 iteration steps.

step is diminished the number of iterations (implicitly that of selections) increases, which leads, in general, to the accumulation of selection errors. Indeed, for a given number of concentration points, an iteration time step that is too small may result in more inaccurate estimations than those obtained for a larger time step. This fact was confirmed by tests on nonreactive models in [13]. In Table I, ΔE_{int} and ΔE_{cin} at $t = 1$ in Case 1 represent the differences between the numerical and exact values ($E_{int} = -8.589$, $E_{cin} = 8.779$) of the internal and kinetic energy, respectively, for different iteration steps p. Here, the kinetic energy was computed as the arithmetic mean of the values obtained from $m = 30$ tests. Note that for the internal energy (which in Case 1 is not affected by random selections) the errors are always improved by diminishing the time step. This is not the case for kinetic energy. At 160 time steps, to improve the error, one has to increase the number of concentration points for the measures associated to the one-particle distribution functions.

The tests also showed that one can still obtain satisfactory results using less concentration points and a larger time step. For example, in Case 1, consider the following values of parameters: (a) 45,000 concentration points and 88 iteration steps (the situation presented in Figs. 1 and 2); (b) 4,500 concentration points and 44 iteration steps. Calculating the maximal error for the kinetic energy δE^a_{cin} and δE^b_{cin} for the situations (a) and (b) respectively,

TABLE I

Errors of Energies for Different Iteration Steps

p	5	10	20	40	80	160
ΔE_{int}	−0.615	−0.290	−0.141	−0.070	−0.035	−0.017
ΔE_{cin}	0.628	0.292	0.155	0.063	0.020	0.059

we obtained the ratio $\delta E^a_{cin}/\delta E^b_{cin} = 0.4644$. Similarly, for the internal energy, $\delta E^a_{int}/\delta E^b_{int} = 0.4604$.

The above remarks also make clear that the accuracy of the numerical scheme requires a proper correlation between the decrease of the time step Δt and the increase in the number n of concentration points of the measures in (45). This fact can be somehow understood from the following considerations, which, although developed for the model presented in Section 2, can be extended to the general case examined in [7].

Let μ and ν be measures of the form (48) and (50) respectively. For some continuous real-valued function ϕ on $\mathbb{R}^3$ define $\bar{\phi} := \int_{\mathbb{R}^3} \phi \, d\mu$. Then, the mean error $es_\phi(\nu, \mu)$ of the approximation of $\bar{\phi}$ by $\int_{\mathbb{R}^3} \phi \, d\nu$ can be evaluated by

$$e_\phi(\nu, \mu) := \left\langle \left| \int_{\mathbb{R}^3} \phi \, d\nu - \int_{\mathbb{R}^3} \phi \, d\mu \right| \right\rangle, \tag{54}$$

where $\langle \ \rangle$ designates the mean with respect to the probability of selection P. First, observe that under the condition $\overline{\phi^2} \leq \infty$, one finds

$$e_\phi(\nu, \mu) \leq \frac{1}{\sqrt{n}} \left[(\overline{\phi^2} - \bar{\phi}^2)^{\frac{1}{2}} + \frac{1}{2} \cdot |\bar{\phi}| \right]. \tag{55}$$

To obtain (55) one applies the Cauchy inequality to the right-hand side of (54), and then one estimates the resulting expression using the definition of P and the independence of the random variables (49).

Then, for $1 \leq p, q \leq J = [[T/\Delta t]]$, define

$$\mathcal{E}_\phi(\nu^{p,J}, \nu^{q,J}) := \max_{1 \leq i \leq N} \left(d_\phi\left(\nu_i^{p,J}, \nu_i^{q,J}\right) \right), \tag{56}$$

with $\nu_i^{p,J}$ as in (47).

Using the properties of collision operators and the estimation (55) in (47), and comparing the iterations on lines $p-1$ and p, it follows that there exist some constants c_1 and c_2 (depending on ϕ, initial data and the parameters of the collision operators in (5)) such that

$$\mathcal{E}_\phi(\nu^{p,J}, \nu^{p-1,J}) \leq \frac{c_1}{\sqrt{n}} (1 + c_2 \Delta t)^{J-p}. \tag{57}$$

Then,

$$\mathcal{E}_\phi(\nu^{J,J}, \nu^{0,J}) \leq \sum_{p=1}^{J} \mathcal{D}_\phi(\nu^{p,J}, \nu^{p-1,J}) \leq \frac{c^T}{\Delta t \sqrt{n}}, \tag{58}$$

where c depends on the same parameters as c_1 and c_2 and T is the final time.

Combining (58) with the estimated contribution of the error due to the time discretization (Proposition 4 of [7]), one obtains an upper bound on the total mean error $\mathcal{E}_{tot,\phi}$ at moment T,

$$\mathcal{E}_{tot,\phi} \leq \delta_{n,T,\Delta t,\phi} + K^T \left(\Delta t + \frac{1}{\Delta t \cdot \sqrt{n}} \right), \tag{59}$$

where the constant K depends on the same parameters as c, while

$$\delta_{n,T,\Delta t,\phi} := \left|\left(\phi, \nu_i^{0,J}\right) - \left(\phi, \nu_i^{J}\right)\right| \tag{60}$$

represents the contribution of the error introduced by the approximation of the initial data. Here ν_i^J and $\nu_i^{0,J}$ are the solutions of the discretized equations (44) for the exact and approximated initial data ν_i^0 and $\nu_i^{0,0}$, respectively.

Obviously $\delta_{n,T,\Delta t,\phi}$ depends on n, T, and Δt through ν_i^J and $\nu_i^{0,J}$ and its behavior depends on the way one approximates the initial data. If one applies low-discrepancy methods, it is known [7] that $\delta_{n,T,\Delta t,\phi} \to 0$ as $n \to \infty$ and $\Delta t \to 0$. However, an explicit estimation on the rapidity of convergence is missing for general models.

Nevertheless, due to the space isotropy of the present model, one can also provide an upper bound for (60). In this respect, we can adapt an argument for the simple gas [10], by comparing (in terms of discrepancy) ν_i^p and $\nu_i^{0,p}$, resulting after p iteration steps from (44), with starting measures ν_i^0 and $\nu_i^{0,0}$, respectively.

To this end, first observe that, without loss of generality, we can consider (59) with $\phi = \phi(v)$ depending only on the radial component of velocity. In the following, we assume that ϕ has bounded variation.

Further, define

$$\mathcal{D}(\nu^{0,p}, \nu^p) := \max_{1\le i\le N}\left(D\left(\nu_i^{0,p}, \nu_i^p\right)\right), \tag{61}$$

where $D(\nu_i^{0,p}, \nu_i^p)$ is the discrepancy (46) of measures $\nu_i^{0,p}$ and ν_i^p. Then observe that (44) implies

$$\begin{aligned}
&\left|\left(\phi_r, \nu_i^{0,p+1}\right) - \left(\phi_r, \nu_i^{p+1}\right)\right| \\
&\quad\le \left|\left(\phi_r, \nu_i^{p}\right) - \left(\phi_r, \nu_i^{p}\right)\right| + \Delta t \sum_{j,k,l=1}^{4} \lambda_{ij,kl} \left| \int_{\mathbb{D}_{ij,kl}} \phi(v)\, d\nu_i^{0,p}(v)\, d\nu_j^{0,p}(w)\, d\zeta\, d\eta \right. \\
&\qquad \left. - \int_{\mathbb{D}_{ij,kl}} \phi(v)\, d\nu_i^{p}(v)\, d\nu_j^{p}(w)\, d\zeta\, d\eta \right| + \Delta t \sum_{j,k,l=1}^{4} \lambda_{kl,ij} \left| \int_{\mathbb{D}_{kl,ij}} \phi_r(\tilde{v}_{kl,ij})\, d\nu_k^{0,p}(v) \right. \\
&\qquad \left. \times\, d\nu_l^{0,p}(w)\, d\zeta\, d\eta - \int_{\mathbb{D}_{kl,ij}} \phi_r(\tilde{v}_{kl,ij})\, d\nu_k^{p}(v)\, d\nu_l^{p}(w)\, d\zeta\, d\eta \right|,
\end{aligned} \tag{62}$$

with ϕ_r the characteristic function of interval $[0, r]$ and $\tilde{v}_{kl,ij}$ given by (28).

Obviously, the first term, and each modulus in the first sum on the right-hand side of (62) are smaller than $\mathcal{D}(\nu^{0,p}, \nu^p)$. To see that the moduli in the last sum of (62) are also smaller than $\mathcal{D}(\nu^{0,p}, \nu^p)$, it is sufficient to remark, in our case, that the applications of the form $v \to \phi_r(\tilde{v}_{kl,ij}(v, w, \zeta, \eta))$ are characteristic functions of a finite union of intervals.

Therefore, from (62) one has

$$\mathcal{D}(\nu^{0,p}, \nu^p) \le (1 + c_0\Delta t) \cdot \mathcal{D}(\nu^{0,p-1}, \nu^{p-1}), \tag{63}$$

with c_0 some constant depending on the same parameters as c_1 and c_2. Then by iterating (63) one finds easily

$$\mathcal{D}(\nu^{0,J}, \nu^J) \leq C_0^T \cdot \mathcal{D}(\nu^{0,0}, \nu^0), \tag{64}$$

with C_0 a constant depending on c_0.

Now, applying the Koksma–Hlavka inequality [9] to (60), and using (64) and the fact that $\mathcal{D}(\nu^{0,0}, \nu^0) = O(\frac{(\log n)^s}{n})$ for some $s > 0$ [9], one finally obtains

$$\mathcal{E}_{tot,\,\phi} \leq K_0^T \frac{(\log n)^s}{n} + K^T \left(\Delta t + \frac{1}{\Delta t \sqrt{n}} \right), \tag{65}$$

where K_0 also depends on the same parameters as c_1 and c_2. The estimations (59) and (65) give some indication how to correlate the choice of the time step with the number of concentration points to control the error, for a given duration of the numerical experiment. An unpleasant feature is the presence of the time step in the denominators of (59) and (65) as a consequence of the accumulation of the errors introduced by selections. This behavior is reflected to some extent by numerical results.

The bounds (59) are not optimal. However, they show that (in the limits of the estimations (59)) the qualitative behavior of the errors is the same, irrespective of the presence of reaction processes in fluids. Nevertheless, the contribution of the Boltzmann terms corresponding to reactions is retained in the rather complicated expressions providing the values of the constants of (58) and (59).

5. CONCLUDING REMARKS

In this paper we presented the implementation of a convergent numerical scheme of the nonlinear Boltzmann model for reacting fluids, where one solves time-discretized equations and the numerical solutions are obtained by iterations alternating with random selections.

The method was applied to a particular space-homogeneous model with binary reactions, for which one can calculate exactly certain macroscopic quantities. The computational effort was $O(n)$, the same as in applications on Boltzmann models for nonreacting multicomponent fluids with elastic Maxwellian collisions [13]. The numerical results indicate good agreement between the computed and exact values of the compared quantities. In particular, the bulk conservation relations are satisfied, on average, in the limit of the numerical errors. Here, it is worth mentioning that, as conjectured in [7], the scheme for reacting fluids does not exhibit (at least numerically) the systematic freezing [4] of the NBI method for a simple gas.

Implementating the scheme for models of reacting gases is more difficult than when modeling simple fluids. Indeed, the integral collision operators involving reaction thresholds are more difficult to evaluate than those corresponding to nonreactive processes, because of the domain integration restrictions in the velocity variables imposed by the energy balance.

Comparing our numerical results with those obtained for a simple gas [13], one can observe the same general behavior of errors. Although not optimal, the upper bound estimations (59) and (65) explain, to some extent, the behavior of different type of errors. Essentially the same dependence on Δt as in the second (expression) term of (65) was obtained using sharp estimations on errors in [10], where a low-discrepancy algorithm was applied to the Krook–Wu version of the classical Boltzmann equation for a monatomic gas.

The error analysis also provides information on the needed correlation between the parameters of the scheme to improve the accuracy of the results.

We recall that the numerical method of [7] can be applied to more general models, with nonconstant collision kernels, with the computational effort being (at most) $O(n \log n)$. Unfortunately, in those situations, it is difficult to find exact solutions. Then the tests should be rather limited to comparing the data provided by the numerical scheme with those obtained from some relevant experiments.

The time discretization applied in this paper is a first-order Euler method. However higher order methods should improve the precision, without increasing the computational effort of the numerical scheme. This could be useful in further computations extending the method to space-dependent problems, by space discretization and application of the space-homogeneous scheme in each space-discretized cell. In this respect, the results of the present paper should be considered as a necessary phase in understanding the simulation in such a space cell. In addition, since the dominant contribution to errors is due to nonlinearities, then we expect (under suitable boundary conditions) that controlling the errors of the simulation in a cell, one could obtain information on the errors of the simulation in the whole domain of space. More specifically, the errors produced by space discretization should behave like those introduced by time discretization, as happens in the NBI scheme for nonhomogeneous monatomic fluids [1]. Moreover, the errors from stochastic selections should accumulate as in the space homogeneous case analyzed in the present paper.

For the same considerations as in Section 3, the weighted selection applied in our numerical experiment could prove its effectiveness in handling space-dependent problems, where one deals with a considerable number of cells, with different concentrations.

Finally observe that directly solving Boltzmann equations by particle methods is useful in describing kinetic low-density regimes. However, this may become extremely expensive in the continuous fluid dynamic limit, where efficient reactive BGK models [11] are more adequate (indeed they skillfully utilize the information that the distribution functions approach local Maxwellians when the mean free path goes to zero). Under these circumstances, for a reacting fluid with various regimes, one could apply a particle method strategy as developed for the simple gas [15], e.g., solving the reactive BGK model when (and where) this is adequate and coupling the solutions to those of the nonlinear Boltzmann model solved in the so-called nonlinear Boltzmann regions [15]. Then an ultimate goal would be to obtain a fluid code able to establish and apply automatically the suitable model, function of the considered space region, and moment of evolution.

ACKNOWLEDGMENTS

We are grateful to the reviewers for their comments which led to considerable improvement of this work. We are also indebted to one of the referees who brought Ref. [11] to our attention.

REFERENCES

1. H. Babovsky and R. Illner, A convergence proof for Nambu's simulation method for the full Boltzmann equation, *SIAM J. Numer. Anal.* **26**, 45 (1989).
2. J. P. Boon, D. Dab, R. Kapral, and A. Lawniczak, Lattice gas automata for reactive systems, *Phys. Rep.* **273**, 55 (1996).

3. A. Ern and V. Giovangigli, *Multicomponent Transport Algorithms*, Lecture Notes in Physics (Springer-Verlag, Berlin, 1994), Vol. 24.
4. C. Greengard and L. G. Reyna, Conservation of expected momentum and energy in Monte Carlo particle simulation, *Phys. Fluids A* **4**, 849 (1992).
5. C. P. Grünfeld, Nonlinear kinetic models with chemical reactions, in *Modeling in Applied Sciences, A Kinetic Theory Approach* edited by N. Bellomo and M. Pulvirenti (Birkhäuser, Boston, 2000), p. 173.
6. C. P. Grünfeld and E. Georgescu, On a class of kinetic equations for reacting gas mixtures, *Mat. Fiz. Anal. Geom.* **2**, 408 (1995).
7. C. P. Grünfeld and D. Marinescu, On the numerical simulation of a class of reactive Boltzmann type equations, *Transp. Theory Stat. Phys.* **26**, 287 (1997).
8. M. Krook and T. T. Wu, Exact solutions of the Boltzmann equations for multicomponents systems, *Phys. Rev. Lett.* **38**, 991 (1977).
9. L. Kuipers and H. Niederreiter, *Uniform Distribution of Sequences* (Wiley, New York, 1974).
10. C. Lécot, A direct simulation Monte Carlo scheme and uniformly distributed sequences for solving the Boltzmann equation. *Computing* **41**, 41 (1989).
11. Y. S. Lian and K. Xu, Gas-kinetic scheme for multimaterial flows and its application in chemical reactions, *J. Comput. Phys.* **163**, 349 (2000).
12. R. Lupini and G. Spiga, Dynamics of a breeding process in a mixture of reacting gases, *Ann. Nucl. Energy* **18**, 197 (1991).
13. D. Marinescu and A. Espesset, Tests of a simulation method for a system of Boltzmann equations, *Comput. Math. Appl.* **40**, 805 (2000).
14. K. Nambu, Direct simulation scheme derived from the Boltzmann equation I. Monocomponent gases, *J. Phys. Soc. Jpn.* **49**, 2042 (1980).
15. H. Neunzert, F. Gropengiesser, and J. Struckmeier, Computational methods for the Boltzmann equation, in *Applied and Industrial Mathematics (Venice, 1989)*, *Math. Appl.*, edited by R. Spigler (Kluwer, Dordrecht, 1991), Vol. 56, p. 111.
16. S. Succi, A. Gabrielli, C. Smith, and E. Kaxiras, Chemical efficiency of reactive microflows with heterogeneous catalysis: A lattice Boltzmann study, preprint (2001); *available at* http://arxiv.org/ps/physics/0103041.
17. J. Struckmaier, Numerical simulation of the Boltzmann equation by particle methods, in *Modeling in Applied Sciences, A Kinetic Theory Approach*, edited by N. Bellomo and M. Pulvirenti (Birkhäuser, Boston, 2000), p. 371.